Polymeric quasicrystal: Mesoscopic quasicrystalline tiling in ABC star polymers

AUTHOR(S):

Hayashida, K; Dotera, T; Takano, A; Matsushita, Y

CITATION:

Hayashida, K ...[et al]. Polymeric quasicrystal: Mesoscopic quasicrystalline tiling in ABC star polymers. Physical Review Letters 2007, 98(19): 195502.

ISSUE DATE:

2007-05-11

URL:

http://hdl.handle.net/2433/50204

Polymeric Quasicrystal: Mesoscopic Quasicrystalline Tiling in *ABC* Star Polymers

Kenichi Hayashida,[1] Tomonari Dotera,[2] Atsushi Takano,[1] and Yushu Matsushita[1]
[1]*Department of Applied Chemistry, Nagoya University, Nagoya 464-8603 Japan*
[2]*Department of Polymer Chemistry, Kyoto University, Kyoto 615-8510, Japan*
(Received 10 January 2007; published 8 May 2007)

A mesoscopic tiling pattern with 12-fold symmetry has been observed in a three-component polymer system composed of polyisoprene, polystyrene, and poly(2-vinylpyridine) which forms a star-shaped terpolymer, and a polystyrene homopolymer blend. Transmission electron microscopy images reveal a nonperiodic tiling pattern covered with equilateral triangles and squares, their triangle/square number ratio of 2.3 ($\approx 4/\sqrt{3}$), and a microbeam x-ray diffraction pattern shows dodecagonal symmetry. The same kind of quasicrystalline structures have been found for metal alloys ($\sim$0.5 nm), chalcogenides ($\sim$2 nm), and liquid crystals ($\sim$10 nm). The present result ($\sim$50 nm) confirms the universal nature of dodecagonal quasicrystals over several hierarchical length scales.

DOI: 10.1103/PhysRevLett.98.195502 PACS numbers: 61.44.Br, 82.35.Jk, 83.80.Uv

The crystallography revolution that occurred in the 1980s was initiated by the discovery of quasiperiodic structures with noncrystallographic rotational symmetry in the field of hard matter [1]. The quasicrystal (QC) state now represents a new class of ordered state distinct from crystal and amorphous material states [2,3]. Soft materials such as phospholipid biomolecules [4], amphiphilic molecules in solutions [5], and block copolymers in condensed systems [6] are commonly known to form a wide variety of self-assembled periodic morphologies. Among these morphologies, *ABC* star-shaped terpolymers produce very complex structures in bulk [7–12] and solution [13]. However, quasicrystalline structures have not yet been observed in any polymeric systems.

The discovery of quasicrystals has provoked much interest in complex tilings composed of sets of nonsingle distinct elements (unit cells). In the case of the dodecagonal quasicrystal (DDQC), unit cells are represented by equilateral triangles and squares [14,15], whose bond angles are multiples of 30 degrees ($=2\pi/12$). This indicates dodecagonal bond orientational order. The use of multiple unit cells in a regular or random fashion enables rearrangement of tiles [16,17]. This additional degree of freedom is known as the phason degree of freedom. A quasicrystalline tiling scheme can vary from an energetically stabilized perfect tiling scheme to an entropically stabilized maximally random tiling scheme with any degree of phason disorder [18]. In entropically stabilized QCs, the entropy stems from dynamic rearrangement of unit cells at high temperatures [19,20]. Furthermore, the entropy has been evaluated by using Bethe ansatz [21].

The first DDQCs were identified within a small particle [22] and in rapid-quenched metals [23]. These QCs were of low quality and unstable with significant phason disorder. Recently, a scaled-up chalcogenide DDQC ($\sim$2 nm) [24,25], and a liquid crystalline one ($\sim$10 nm) have been found [26]. Moreover, it has been elucidated that even when tile rearrangement is frozen in bulk, the maximal entropy state of a random tiling is accecible through growth alone [27]. In any case, the existence of equilateral triangles and squares within a structure may provide the route to formation of dodecagonal quasicrystals.

It was recently found that polymeric stars tend to form cylinder-based structures whose cross-sections reveal two-dimensional tiling patterns as shown schematically in Fig. 1. The peculiar feature of the bulk structures of those molecules arises from having junction points aligned on lines if the three-component polymers are immiscible with one another. In a polymeric star of the type $I_{1.0}S_{1.0}P_{1.3}$, where I, S, and P denote polyisoprene, polystyrene, and poly(2-vinylpyridine), respectively, we found an Archimedean tiling structure (3.3.4.3.4) [28,29] composed of triangles (Tri.) and squares (Sq.), with all vertices surrounded by a Tri.-Tri.-Sq.-Tri.-Sq. tiling pattern. Furthermore, the same tiling pattern was found in an $I_{1.0}S_{2.3}P_{2.0}$ blend [30], which was actually an *ISP* star-branched molecule/

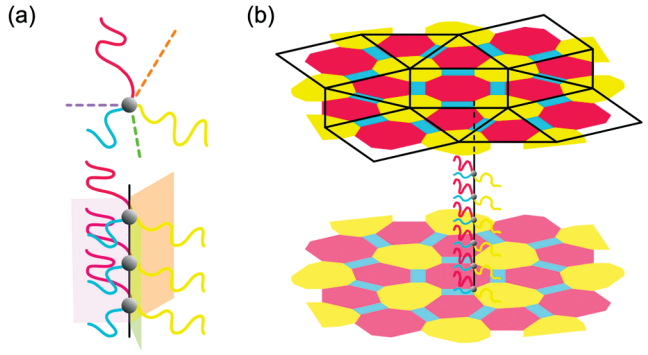

FIG. 1 (color). Schematic drawings of the intramolecular phase separation of *ABC* star-shaped terpolymer chains in bulk (a) and their nanodomain assembly (b). When the three phase-separated components are strongly incompatible with one another, the junction points are aligned on lines in bulk. Accordingly, the components tend to form microphase-separated structures with cylinder-based morphology.

S-homopolymer blend, where a low molecular weight homopolymer can play a role in controlling the volume fraction of the system.

It should be noted that (3.3.4.3.4) is a crystalline analog of a QC and is known as the σ phase in the Frank-Kasper complex crystalline alloy family [31]. In every other system with a different length scale, it is known that both (3.3.4.3.4) and dodecagonal phases always appear with a slight composition change. In (3.3.4.3.4), the N_3/N_4 ratio is exactly two, where N_3 and N_4 represent the numbers of triangles and squares. If we increase the ratio by varying the polymer composition, we obtain the DDQC, where the definitive N_3/N_4 ratio should be at about 2.31 ($\approx 4/\sqrt{3}$).

A quasi-two-dimensional Monte Carlo simulation and mean field theories suggest the existence of equilibrium QCs [32–34]. However, the equilibrium state appears to be experimentally difficult to achieve. The system favors cylindrical morphology, and, therefore, tile rearrangement in plane and in the c axis may be quite slow in the attainable temperature range. In fact, by exploring a composition range in the vicinity of the (3.3.4.3.4) structure, we have reached a kinetically-frozen tiling pattern with dodecagonal symmetry as shown below.

The polymer samples were prepared using a previously-described anionic polymerization process [30]. Two parent ISP terpolymers, i.e., $I_{1.0}S_{1.8}P_{2.0}$ and $I_{1.0}S_{1.8}P_{2.5}$, and a 3k styrene homopolymer were blended to produce $I_{1.0}S_{2.3}P_{2.0}$ and $I_{1.0}S_{2.7}P_{2.5}$. The films used for morphological observations were obtained by casting, drying, and annealing at 170 °C for three days. Transmission electron microscopy (TEM) and small-angle x-ray scattering (SAXS) experiments were performed as described previously [28,30].

Figures 2(a) and 2(b) compare the typical bright field TEM images observed for $I_{1.0}S_{2.3}P_{2.0}$ and $I_{1.0}S_{2.7}P_{2.5}$. Figure 2(a) indicates a periodic pattern assigned as (3.3.4.3.4), while the pattern shown in Fig. 2(b) is significantly complex. The square-triangle lattice is superimposed in Figs. 2(c) and 2(d) by placement of a vertex on the center of each poly(2-vinylpyridine) domain. The tiling pattern shown in Fig. 2(d) is different from that of 2(c). Observations should be made on a wider area to elucidate the regularity that governs the pattern.

The wider TEM image is shown in Fig. 3(a), again with square-triangle tiling superimposed upon the image. In order to analyze the arrangement of tiles in this figure, the tessellation within the sample range containing four dislocations was transcribed into the tiling pattern with regular triangles and squares in Fig. 3(b). Note that in cases where there are strong perturbations in the vicinity of a dislocation, the transcription to triangles and squares was suspended. The numbers of triangles and squares are 461 and 200, respectively, with 503 vertices within the area in Fig. 3(b) with a triangle/square ratio of 2.305, which is close to the ideal value of 2.309 ($\approx 4/\sqrt{3}$) for a quasiperiodic tiling pattern with dodecagonal symmetry. Two types

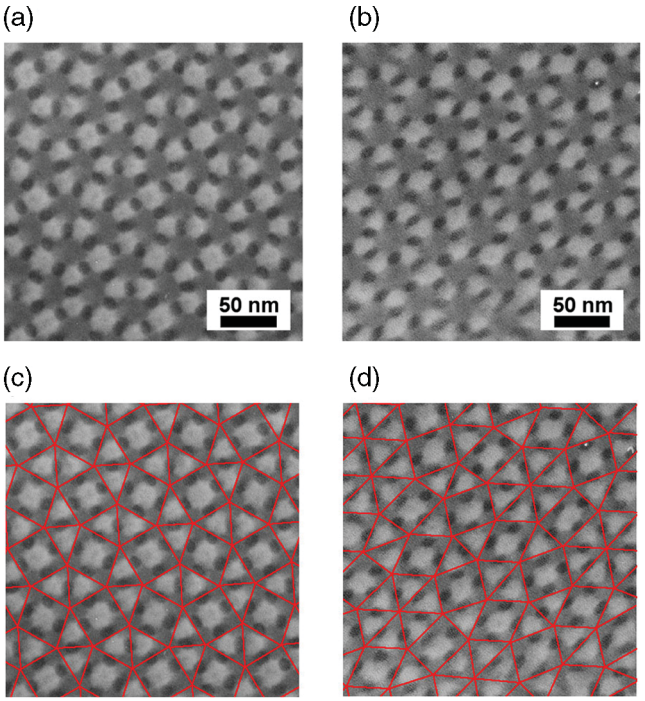

FIG. 2 (color). Typical bright field transmission electron micrographs obtained for ISP terpolymer /S homopolymer blend system: polyisoprene (I, black), polystyrene (S, white), and poly(2-vinylpyridine) (P, gray). The polymer samples are (a) $I_{1.0}S_{2.3}P_{2.0}$ and (b) $I_{1.0}S_{2.7}P_{2.5}$. The imaginary equilateral triangle (Tri) and square (Sq) are superimposed on the images in (c) and (d), respectively. In Fig. 2(c), each vertex is surrounded by Tri.- Tri.- Sq.- Tri.- Sq., so that (3.3.4.3.4) Archimedean tiling holds for the self-assembled structure. In Fig. 2(d), there is no periodicity observed in the arrangement of the square-triangle tiling.

of periodic portions as ''approximants'' are shown in color in Fig. 3(b). One approximant, i.e., the (3.3.4.3.4) Archimedean tiling pattern, has a $p4gm$ plane group. The other one is an 8/3 approximant with 6-fold symmetry whose plane group is $p6mm$. The N_3/N_4 ratio of the latter is 8/3 (≈ 2.667). Since bond orientational order exists, the direction of domains can be classified into three orientations (shown in brown, pink, and violet) for (3.3.4.3.4) tiling, and two (yellow and green) for 8/3 approximants, while the transition regions are shown in white. We find that these colored regions are distributed in a random manner.

The diffracted intensity map obtained by the microbeam SAXS experiment is shown in Fig. 4(a). The microbeam SAXS measurements were performed for annealed sample films using beam line BL40XU at the SPring-8 facility. The wavelength of the x-ray used was 0.12 nm, and the size of the collimated beam was approximately 5 μm $\times$ 5 μm (FWHM), with a camera length of 2.75 m. The dodecagonal pattern up to the higher order can be recognized from the magnitudes of nonidentical intensities. The average of

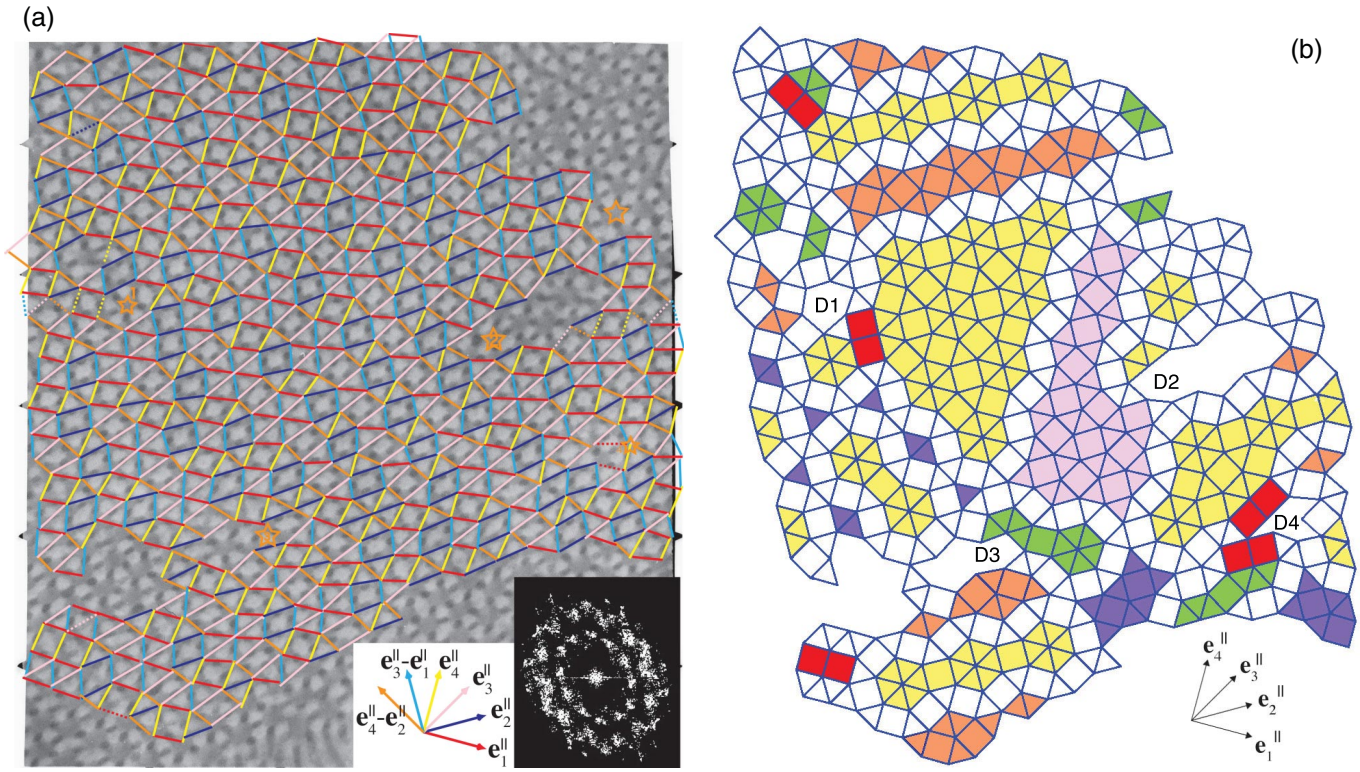

FIG. 3 (color). (a) Observed square-triangle tiling. The imaginary tiling is superimposed on the TEM image which covers a much wider area than that of Fig. 2(b). The FFT pattern from the TEM staining contrasts is also shown. (b) Transcribed tiling obtained by transcribing the tile tessellation style in Fig. 3(a) using regular triangles and squares. To remove mismatches around dislocation cores D1-D4, vertex positions are corrected by using Burgers vectors. The numbers of triangles and squares are 461 and 200, respectively, with a triangle/square ratio of 2.305, which is close to the ideal value of 2.309 ($=4/\sqrt{3}$) for dodecagonal quasicrystals. Two types of approximants (3.3.4.3.4) (brown, pink, and violet) and 8/3 (yellow and green) are shown in colors according to their orientation, while transition regions are in white, and consecutive squares are in red.

the magnitude of the prominent scattering vectors, $|q|$, is 0.149 nm^{-1}, and hence the length of sides of triangles and squares, l, is estimated to be 47.0 nm, according to the relationship, $l = 2\pi\sqrt{2+\sqrt{3}}/(\sqrt{3}|q|)$ [35]. This value is in good agreement with the TEM result shown in Fig. 2(b).

In contrast to this two-dimensional image observed in reciprocal space, Fourier transformation was carried out using only the vertex data for Fig. 3(b). The result is displayed in Fig. 4(b). The dodecagonal symmetry pattern can be seen again, and we note that the observed diffraction image in Fig. 4(a) agrees surprisingly well with the image based on the real space data. The relative magnitudes of all 12 spots are not identical. Eight of them are stronger, and four of them are weaker. This can be attributed to frozen dislocations and possibly the nonuniformity of orientations and the various sizes of two approximants in the microbeam region.

To investigate the existence of dodecagonal quasiperiodic translational order, we evaluated the phason strain of the tiling in terms of higher dimensional (projection) method [19,20], in which a DDQC is obtained by projection from a four-dimensional hyperlattice onto the physical space. Assuming that $\boldsymbol{e}_i^{\parallel}$ and $\boldsymbol{e}_i^{\perp}$ are projections of the basis vectors of the hyperspace onto two orthogonal subspaces, physical (parallel), and perpendicular spaces, respectively, all tiling vertices can be described by $\boldsymbol{r}^{\parallel} = \sum_{i=1}^{4} n_i \boldsymbol{e}_i^{\parallel}$, where $\boldsymbol{e}_i^{\parallel} = (\cos[\pi i/6], \sin[\pi i/6])$ as shown in Fig. 3(b)

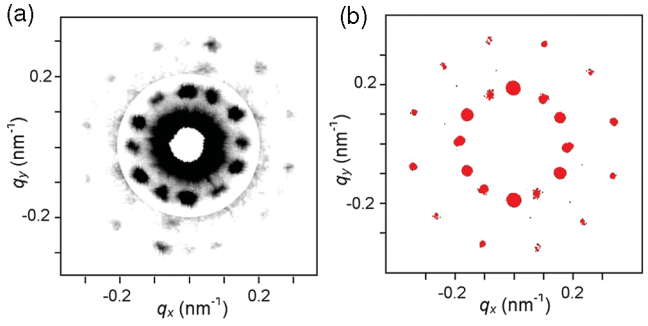

FIG. 4 (color). (a) The microbeam small-angle x-ray scattering pattern obtained for the annealed sample film of $I_{1.0}S_{2.7}P_{2.5}$ with approximately 30 μm thickness. The intensities of the outer 12 diffraction peaks are scaled up by a factor of 10. (b) The simulated diffraction pattern for Fig. 3(b) displaying only peaks above an arbitrary intensity. The radii of circles are proportional to their intensities.

TABLE I. Invariant representation of phason strain.

	$\lvert\alpha\rvert$	$\lvert\beta\rvert$	$\sqrt{\gamma^2+\mu^2}$
(3.3.4.3.4)	0.000	0.000	0.268
8/3	0.259	0.0693	0.000
Sample	0.0486	0.00720	0.0319

and the n_i values are integers. The corresponding position in the perpendicular space is defined by $\boldsymbol{r}^{\perp} = \sum_{i=1}^{4} n_i \boldsymbol{e}_i^{\perp}$, where $\boldsymbol{e}_i^{\perp} = (\cos[7\pi i/6], \sin[7\pi i/6])$. Then, the phason strain matrix $\boldsymbol{A} = \nabla_{\parallel} \boldsymbol{r}^{\perp}$ is calculated by linear-square fitting to $\boldsymbol{r}^{\perp} \cong \boldsymbol{A}\boldsymbol{r}^{\parallel}$ over entire vertices. While DDQCs should give $\boldsymbol{A} = \boldsymbol{0}$, approximants give certain constant values depending on the degree of approximation to QCs. Since the sample contains four dislocations (D1-D4 in Fig. 3(b) [36]), we need to correct both the physical and perpendicular positions to eliminate jumps (tears) in both spaces [19].

In Table I, the components of $\boldsymbol{A}$ in terms of the invariant representation under a rotation of $(2\pi/12)$,

$$\boldsymbol{A} = \begin{pmatrix} \alpha+\gamma & -\beta+\mu \\ \beta+\mu & \alpha-\gamma \end{pmatrix}, \tag{1}$$

for two approximants and the sample are compared. $|\alpha|$ of an 8/3 approximant and $\sqrt{\gamma^2+\mu^2}$ of a (3.3.4.3.4) approximant are of the order of 0.1, while both observed values for the present sample are of the order of 0.01, which implies that the global linear phason is quite small.

To summarize, the observed tiling pattern possesses essential features of a quasicrystal with dodecagonal symmetry in the mesoscopic length scale, although the extent of quasicrystalline order is a few microns. Many local defects and dislocations may be due to the kinetic nature of the present sample, and we expect the existence of a stable QC if hysteresis is removed by long-term thermal annealing or if the compositions of component polymers are varied slightly. Concerning the origin of quasicrystalline order, growth mechanism is, in particular, of interest, and disordering along cylindrical axis required by entropic stability should be addressed in future.

The present result indicates the universality of the dodecagonal symmetry pattern, covering a wide variety of materials including metallic alloys, chalcogenides, organic dendrons, and the present polymeric star system. We expect that this finding will stimulate both polymer sciences and the research of quasicrystals.

This work was mainly supported by a Grant-in-Aid for the Basic Research A (No. 17205021) from MEXT, Japan. The SAXS experiments were performed under SPring-8, Proposal No. 2005A0221. K. H. and Y. M. were supported by the 21st century COE program entitled "The creation of Nature Guided Materials Processing." A. T. was supported by PRESTO, JST. T. D. is grateful to Chris L. Henley for thoughtful comments.

[1] D. Shechtman *et al.*, Phys. Rev. Lett. **53**, 1951 (1984).
[2] D. Levine and P. J. Steinhardt, Phys. Rev. Lett. **53**, 2477 (1984).
[3] A. P. Tsai, A. Inoue, and T. Masumoto, Jpn. J. Appl. Phys. **26**, L1505 (1987).
[4] G. Lindblom *et al.*, J. Am. Chem. Soc. **101**, 5465 (1979).
[5] P. Alexandridis, U. Olsson, and B. Lindman, Langmuir **13**, 23 (1997).
[6] E. L. Thomas *et al.*, Nature (London) **334**, 598 (1988).
[7] T. Fujimoto *et al.*, Polymer **33**, 2208 (1992).
[8] S. Sioula, N. Hadjichristidis, and E. L. Thomas, Macromolecules **31**, 8429 (1998).
[9] H. Hückstädt, A. Göpfert, and V. Abetz, Macromol. Chem. Phys. **201**, 296 (2000).
[10] Y. Bohbot-Raviv and Z.-G. Wang, Phys. Rev. Lett. **85**, 3428 (2000).
[11] T. Gemma, A. Hatano, and T. Dotera, Macromolecules **35**, 3225 (2002).
[12] A. Takano *et al.*, Macromolecules **37**, 9941 (2004).
[13] Z. Li *et al.*, Science **306**, 98 (2004).
[14] P. Stampfli, Helv. Phys. Acta **59**, 1260 (1986).
[15] K. Niizeki and H. Mitani, J. Phys. A **20**, L405 (1987).
[16] K. Kawamura, Prog. Theor. Phys. **70**, 352 (1983).
[17] V. Elser, Phys. Rev. Lett. **54**, 1730 (1985).
[18] T. Dotera and P. J. Steinhardt, Phys. Rev. Lett. **72**, 1670 (1994).
[19] P. W. Leung, C. L. Henley, and G. V. Chester, Phys. Rev. B **39**, 446 (1989).
[20] M. Oxborrow and C. L. Henley, Phys. Rev. B **48**, 6966 (1993).
[21] M. Widom, Phys. Rev. Lett. **70**, 2094 (1993).
[22] T. Ishimasa, H.-U. Nissen, and Y. Fukano, Phys. Rev. Lett. **55**, 511 (1985).
[23] H. Chen, D. X. Li, and K. H. Kuo, Phys. Rev. Lett. **60**, 1645 (1988).
[24] M. Conrad, F. Krumeich, and B. Harbrecht, Angew. Chem., Int. Ed. **37**, 1383 (1998).
[25] A. Yamamoto, Acta Crystallogr. Sect. A **60**, 142 (2004).
[26] X. Zeng *et al.*, Nature (London) **428**, 157 (2004).
[27] D. Joseph and V. Elser, Phys. Rev. Lett. **79**, 1066 (1997).
[28] A. Takano *et al.*, J. Polym. Sci., Part B: Polym. Phys. **43**, 2427 (2005).
[29] K. Hayashida *et al.*, Macromolecules **39**, 4869 (2006).
[30] K. Hayashida *et al.*, Macromolecules **39**, 9402 (2006).
[31] F. C. Frank and J. S. Kasper, Acta Crystallogr. **12**, 483 (1959).
[32] T. Dotera and T. Gemma, Philos. Mag. **86**, 1085 (2006).
[33] R. Lifshitz and D. M. Petrich, Phys. Rev. Lett. **79**, 1261 (1997).
[34] T. Dotera, Philos. Mag. (to be published).
[35] Q. B. Yang and W. D. Wei, Phys. Rev. Lett. **58**, 1020 (1987).
[36] Burgers vector is defined as the sum of lattice vectors along the clockwise circuit around a dislocation: D1 (1, 0, −1, 1), D2 (−1, 0, 1, 0), D3 (0, 1, −1, 0), D4 (0, −1, 1, −1).